Statistical Characterization of *Eigen*-Channels in Time-Varying Rayleigh Flat Fading MIMO Systems

Shuangquan Wang, Ali Abdi

Center for Wireless Communications and Signal Processing Research
Department of Electrical and Computer Engineering
New Jersey Institute of Technology, Newark, New Jersey 07102
Email: sw27@njit.edu; ali.abdi@njit.edu

***Abstract*— In this paper, some important second-order statistics such as the correlation coefficient, level crossing rate, and average fade duration of *eigen*-channels, are studied, in time-varying Rayleigh multiple-input multiple-output (MIMO) channels, assuming a general *non-isotropic* scattering environment. Exact closed-form expressions are derived and Monte Carlo simulations are provided to verify the accuracy of the analytical results. These results serve as useful tools for analysis and design of MIMO systems in time-varying channels.**

I. Introduction

The utilization of antenna arrays at the base station (BS) and the mobile station (MS) in a wireless communication system increases the capacity linearly with $\min(N_T, N_R)$, where N_T and N_R are numbers of transmit and receive antenna elements, respectively, provided that the environment is sufficiently rich in multi-path components [1][2]. This is due to the fact that a multiple-input multiple-output (MIMO) channel can be decomposed to several parallel single-input single-output (SISO) channels, called *eigen*-channels or *eigen*-modes, via the singular value decomposition (SVD) [2]–[9].

For a SISO channel, or any subchannel[1] of a MIMO system, there are numerous studies on key second-order statistics such as correlation, level crossing rate (LCR), and average fade duration (AFD) [10]–[14]. However, to the best of our knowledge, no such study on the *eigen*-channels of a MIMO system is reported in the literature, mainly due to the lack of knowledge regarding the joint probability density function (PDF) of *eigen*-channels. These statistics will provide useful metrics for designing the adaptive transmission scheme over *eigen*-channels.

In this paper, a number of second-order statistics such as the autocorrelation function (ACF), correlation coefficient, LCR and AFD of *eigen*-channels are studied in MIMO time-varying Rayleigh flat fading channels. We assume all the subchannels are spatially independent and identically distributed (i.i.d.), with the same temporal correlation coefficient, considering general *non-isotropic* scattering propagation environments. Closed-form expressions are derived, and Monte Carlo simulations are provided to verify the accuracy of our closed-form expressions.

[1]In this paper, each subchannel represents the radio link between each transmit/receive pair of antennas.

Notation: $\cdot^\dagger$ is reserved for matrix Hermitian, $\cdot^\star$ for complex conjugate, $\jmath$ for $\sqrt{-1}$, $\mathbb{E}[\cdot]$ for mathematical expectation, $\mathbf{I}_m$ for the $m \times m$ identity matrix, $\|\cdot\|_F$ for the Frobenius norm, $\Re[\cdot]$ and $\Im[\cdot]$ for the real and imaginary parts of a complex number, respectively, and $f^2(x)$ for $[f(x)]^2$. Finally, $t \in [m, n]$ implies that t, m and n are integers such that $m \le t \le n$ with $m \le n$.

The rest of this paper is organized as follows. Sec. II introduces the channel model, as well as the angle-of-arrival (AoA) model. *Eigen*-channels of a MIMO system are discussed in Sec. III. Sec. IV is devoted to the derivation of the normalized ACF (NACF) and correlation coefficient the *eigen*-channels of a 2×2 MIMO system, whereas Sec. V focuses on LCR and AFD of the *eigen*-channels. Numerical results are presented in Sec. VI, and concluding remarks are given in Sec. VII.

II. Channel Model

In this paper, an $N_R \times N_T$ MIMO time-varying Rayleigh flat fading channel is considered. Similar to [15], we consider a piecewise constant approximation for the continuous-time MIMO fading channel matrix coefficient $\mathbf{H}(t)$, represented by $\{\mathbf{H}(lT_s)\}_{l=1}^{L}$, where T_s is the symbol duration and L is the number of samples. In the l^{th} symbol duration, the matrix of channel coefficients is given by

$$\mathbf{H}(lT_s) = \begin{bmatrix} h_{1,1}(lT_s) & \cdots & h_{1,N_T}(lT_s) \\ \vdots & \ddots & \vdots \\ h_{N_R,1}(lT_s) & \cdots & h_{N_R,N_T}(lT_s) \end{bmatrix}, l \in [1, L]. \quad (1)$$

We assume all the $N_T N_R$ subchannels $\{h_{n_r,n_t}(lT_s), l \in [1, L]\}_{(n_r=1,n_t=1)}^{(N_R,N_T)}$ are i.i.d., with the same temporal correlation coefficient, i.e.,

$$\mathbb{E}[h_{mn}(lT_s) h_{pq}^\star((l-i)T_s)] = \delta_{mp}\delta_{nq}\rho_h(iT_s), \quad (2)$$

where the Kronecker delta δ_{mp} is 1 or 0 when $m = p$ or $m \ne p$, respectively, and $\rho_h(iT_s)$ is derived at the end of this section, eq. (6).

In flat Rayleigh fading channels, each $h_{n_r,n_t}(lT_s), l \in [1, L]$, is a zero-mean complex Gaussian random process. In the l^{th} interval, $h_{n_r,n_t}(lT_s)$ can be represented as [13]

$$\begin{aligned} h_{n_r,n_t}(lT_s) &= h_{n_r,n_t}^I(lT_s) + \jmath h_{n_r,n_t}^Q(lT_s), \\ &= \alpha_{n_r,n_t}(lT_s) \exp[-\jmath \Phi_{n_r,n_t}(lT_s)], \end{aligned} \quad (3)$$

$$p(x,y)=\frac{(xy)^{\frac{\nu}{2}}e^{-\frac{x+y}{1-\varrho_i^2}}I_\nu\left(\frac{2\varrho_i\sqrt{xy}}{1-\varrho_i^2}\right)}{M^2(1-\varrho_i^2)\varrho_i^\nu}\sum_{k=0}^{M-1}\frac{k!L_k^\nu(x)L_k^\nu(y)}{(k+\nu)!\varrho_i^{2k}}+\frac{(xy)^\nu e^{-(x+y)}}{M^2}\sum_{0\le k<l}^{M-1}\Bigg\{\frac{k!l!}{(k+\nu)!(l+\nu)!}$$
$$\times\left\{\left[L_k^\nu(x)L_l^\nu(y)\right]^2+\left[L_l^\nu(x)L_k^\nu(y)\right]^2-\left[\varrho_i^{2(l-k)}+\varrho_i^{2(k-l)}\right]L_k^\nu(x)L_l^\nu(x)L_k^\nu(y)L_l^\nu(y)\right\}\Bigg\}. \quad (4)$$

$$p(x,y)=\frac{e^{-(x+y)}}{4\varrho_i^2}\left\{\frac{\varrho_i^2-x+y(x-1)+1}{1-\varrho_i^2}\exp\!\left[-\frac{\varrho_i^2(x+y)}{1-\varrho_i^2}\right]I_0\!\left(\frac{2\varrho_i\sqrt{xy}}{1-\varrho_i^2}\right)-\left(y\varrho_i^2-\varrho_i^2-x+1\right)\left(x\varrho_i^2-\varrho_i^2-y+1\right)\right\},\quad x,y\ge 0. \quad (5)$$

where the zero-mean real Gaussian random processes $h^I_{n_r,n_t}(lT_s)$ and $h^Q_{n_r,n_t}(lT_s)$ are the real and imaginary parts of $h_{n_r,n_t}(lT_s)$, respectively. $\alpha_{n_r,n_t}(lT_s)$ is the envelope of $h_{n_r,n_t}(lT_s)$ and $\Phi_{n_r,n_t}(lT_s)$ is the phase of $h_{n_r,n_t}(lT_s)$. For each l, $\alpha_{n_r,n_t}(lT_s)$ has a Rayleigh distribution and $\Phi_{n_r,n_t}(lT_s)$ is distributed uniformly over $[-\pi,\pi)$. Without loss of generality, we assume each subchannel has unit power, i.e., $\mathbb{E}[\alpha^2_{n_r,n_t}(lT_s)]=1$.

Using the empirically-verified [13] multiple von Mises PDF [16, (4)] for the AoA at the receiver in *non-isotropic* scattering environments, shown as Fig. 1 of [16], the channel correlation coefficient of $h_{n_r,n_t}(lT_s)$, $\forall n_r,n_t$, is given by [16, (7)]

$$\begin{aligned}\rho_h(iT_s)&=\mathbb{E}[h_{n_r,n_t}(lT_s)h^\star_{n_r,n_t}((l-i)T_s)],\\ &=\sum_{n=1}^{N}P_n\frac{I_0\!\left(\sqrt{\kappa_n^2-4\pi^2f_D^2i^2T_s^2+\jmath 4\pi\kappa_n f_D iT_s\cos\theta_n}\right)}{I_0(\kappa_n)},\end{aligned}\quad (6)$$

where $I_k(z)=\frac{1}{\pi}\int_0^\pi e^{z\cos\theta}\cos(k\theta)\mathrm{d}\theta$ is the k^{th} order modified Bessel function of the first kind. θ_n is the mean AoA of the n^{th} cluster of scatterers, κ_n controls the width of the n^{th} cluster of scatterers, P_n represents the contribution of the n^{th} cluster of scatterers such that $\sum_{n=1}^N P_n=1, 0<P_n\leqslant 1$, N is the number of clusters of scatterers, and f_D is the maximum Doppler frequency. When $\kappa_n=0,\forall n$, which corresponds to *isotropic* scattering, (6) reduces to $\rho_h(iT_s)=I_0(\jmath 2\pi f_D iT_s)=J_0(2\pi f_D iT_s)$ [16], which is the Clarke's correlation model.

III. Eigen-Channels in MIMO Systems

We set $M=\min(N_T,N_R)$ and $N=\max(N_T,N_R)$. Based on singular value decomposition (SVD) [2]–[9], $\mathbf{H}(lT_s)$ in (1) can be diagonalized in the following form

$$\mathbf{H}(lT_s)=\mathbf{U}(lT_s)\mathbf{S}(lT_s)\mathbf{V}^\dagger(lT_s), \quad (7)$$

where $\mathbf{V}(lT_s)$, whose dimension is $N_T\times M$, satisfies $\mathbf{V}^\dagger(lT_s)\mathbf{V}(lT_s)=\mathbf{I}_M$, $\mathbf{U}(lT_s)$, which is $N_R\times M$, satisfies $\mathbf{U}^\dagger(lT_s)\mathbf{U}(lT_s)=\mathbf{I}_M$, and $\mathbf{S}(lT_s)$ is a diagonal matrix, given by $\mathbf{S}(lT_s)=\mathrm{diag}\left[s_1(lT_s),\cdots,s_M(lT_s)\right]$, in which $s_m(lT_s)$, $m\in[1,M]$ is the m^{th} non-zero singular value of $\mathbf{H}(lT_s)$.

We define $\lambda_m(lT_s)=s_m^2(lT_s)$, $\forall m$. Therefore $\lambda_m(lT_s)$ is the m^{th} non-zero eigenvalue of $\mathbf{H}(lT_s)\mathbf{H}^\dagger(lT_s)$. We further consider $\{\lambda_m(lT_s)\}_{m=1}^M$ as unordered non-zero eigenvalues of $\mathbf{H}(lT_s)\mathbf{H}^\dagger(lT_s)$. Therefore the MIMO channel $\mathbf{H}(lT_s)$ is decomposed into M identically distributed[2] *eigen*-channels, $\{\lambda_m(lT_s), l\in[1,L]\}_{m=1}^M$, by SVD, as shown in Fig. 1. For $M=1$, there is only one *eigen*-channel, which corresponds to the maximum ratio transmitter (MRT) if $N_R=1$, or the maximum ratio combiner (MRC) if $N_T=1$. In each case we have N i.i.d complex Gaussian branches.

Since all the *eigen*-channels have identical statistics, we only study one of them and denote it as $\lambda(lT_s), l\in[1,L]$. To simplify the notation, we use X and Y to denote $\lambda(lT_s)$ and $\lambda((l-i)T_s)$, respectively. The joint PDF of X and Y is given in (4) [17], where $L_n^\alpha(x)=\frac{1}{n!}e^x x^{-\alpha}\frac{\mathrm{d}^n}{\mathrm{d}x^n}\left(e^{-x}x^{n+\alpha}\right)$ is the associated Laguerre polynomial of order n [18, pp. 1061, 8.970.1], $\nu=N-M$, and $\varrho_i=|\rho_h(iT_s)|$, where $\rho_h(iT_s)$ is given in (6). The joint PDF in (4) is very general and includes many existing PDF's as special cases.

- By integration over y, (4) reduces to the marginal PDF

$$p(x)=\frac{1}{M}\sum_{m=0}^{M-1}\frac{m!}{(m+\nu)!}\left[L_m^\nu(x)\right]^2x^\nu e^{-x}, \quad (8)$$

which is the same as the PDF presented in [2]. When $M=1$, (8) further reduces to

$$p(x)=\frac{1}{(N-1)!}x^{N-1}e^{-x}, \quad (9)$$

which is the χ^2 distribution with $2N$ degrees of freedom [19, (2.32)], used for characterizing the PDF of outputs of MRT or MRC.

- With $M=1$, (4) reduces to

$$p(x,y)=\frac{(xy)^{\frac{N-1}{2}}\exp\left(-\frac{x+y}{1-\varrho_i^2}\right)I_{N-1}\left(\frac{2\varrho_i\sqrt{xy}}{1-\varrho_i^2}\right)}{(N-1)!\left(1-\varrho_i^2\right)\varrho_i^{N-1}}, \quad (10)$$

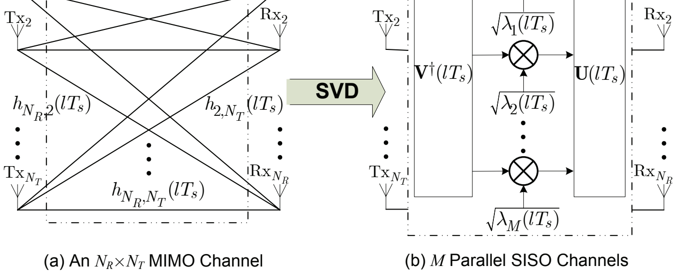

Fig. 1. (a) A MIMO channel with N_T transmit and N_R receive antennas; (b) The equivalent M parallel SISO channels.

[2] In general, the eigen-channels are correlated.

which is the joint PDF of outputs of MRT or MRC at the $l^{\rm th}$ and $(l-i)^{\rm th}$ symbol durations [20]. Furthermore, when $N=1$, i.e., a SISO channel, (10) simplifies to

$$p(x,y)=\frac{1}{1-\varrho_i^2}\exp\left(-\frac{x+y}{1-\varrho_i^2}\right)I_0\left(\frac{2\varrho_i\sqrt{xy}}{1-\varrho_i^2}\right), \quad (11)$$

which is identical to (8-103) [21, pp. 163] after a one-to-one nonlinear mapping.

In the following sections, the normalized autocorrelation, correlation coefficient, LCR and AFD of an *eigen*-channel $\lambda(lT_s), l\in[1,L]$ are investigated for a 2×2 MIMO system[3], where the joint PDF is given in (5), after plugging $M=2$ and $\nu=0$ into (4).

IV. NACF and Correlation Coefficient of an Eigen-Channel

In this section, first we concentrate on the ACF of an *eigen*-channel $\lambda(lT_s), l\in[1,L]$. The ACF is defined by

$$\begin{aligned} r_\lambda(i)&=\mathbb{E}[\lambda(lT_s)\lambda((l-i)T_s)],\\ &=\int_0^\infty\int_0^\infty xy\,p(x,y)\mathrm{d}x\mathrm{d}y, \end{aligned} \quad (13)$$

where $p(x,y)$ is given by (5).

Combining (5) with the following Taylor series [18, pp. 971, 8.447.1]

$$I_0(t)=\sum_{k=0}^\infty\frac{t^{2k}}{(k!)^2 2^{2k}}, \quad (14)$$

we simplify (13) to

$$r_\lambda(i)=\begin{cases}8, & i=0,\\ 4+\varrho_i^2, & i\neq 0,\end{cases} \quad (15)$$

where the second moment of X, $r_\lambda(0)$, is calculated as $\mathbb{E}[X^2]$ directly, using the PDF of X, which can be derived from (8) by replacing M with 2

$$p(x)=\left(\frac{x^2}{2}-x+1\right)e^{-x}, x\geq 0. \quad (16)$$

From (15), we can easily get NACF as

$$\boxed{\tilde{r}_\lambda(i)=\frac{r_\lambda(i)}{\mathbb{E}[X^2]}=\begin{cases}1, & i=0,\\ \frac{1}{2}+\frac{\varrho_i^2}{8}, & i\neq 0.\end{cases}} \quad (17)$$

With $\mathbb{E}[X]=2$, the mean of X, which is easily calculated using (16), the correlation coefficient is given by

$$\boxed{\rho_\lambda(i)=\frac{r_\lambda(i)-\{\mathbb{E}[X]\}^2}{\mathbb{E}[X^2]-\{\mathbb{E}[X]\}^2}=\begin{cases}1, & i=0,\\ \frac{\varrho_i^2}{4}, & i\neq 0.\end{cases}} \quad (18)$$

From (17) and (18), it is interesting to observe that NACF and the correlation coefficient are not continuous at $i=0$, as $\tilde{r}_\lambda(1)$ and $\rho_\lambda(1)$ do not converge to $\tilde{r}_\lambda(0)=\rho_\lambda(0)=1$ as $T_s\to 0$.

[3]Other configurations can be handled via the same techniques developed in this paper, and using the joint PDF in (4). The 2×2 case is emphasized in this paper to provide further insight, rather than lengthy equations.

With isotropic scattering, (17) and (18), respectively, reduce to

$$\tilde{r}_\lambda(i)=\begin{cases}1, & i=0,\\ \frac{1}{2}+\frac{J_0^2(2\pi f_D iT_s)}{8}, & i\neq 0,\end{cases} \quad (19)$$

and

$$\rho_\lambda(i)=\begin{cases}1, & i=0,\\ \frac{J_0^2(2\pi f_D iT_s)}{4}, & i\neq 0.\end{cases} \quad (20)$$

V. LCR and AFD of an Eigen-Channel

A. LCR of an Eigen-Channel

Similar to the calculation of zero crossing rate in discrete time [22, Ch. 4], we define the binary sequence $\{Z_l\}_{l=1}^L$, based on the *eigen*-channel samples $\{\lambda(lT_s)\}_{l=1}^L$, as

$$Z_l=\begin{cases}1, & \text{if } \lambda(lT_s)\geq\lambda_{\rm th},\\ 0, & \text{if } \lambda(lT_s)<\lambda_{\rm th},\end{cases} \quad (21)$$

where $\lambda_{\rm th}$ is a fixed threshold. The number of crossings of $\{\lambda(lT_s)\}_{l=1}^L$ with $\lambda_{\rm th}$, within the time interval $T_s\leq t\leq LT_s$, denoted by $D_{\lambda_{\rm th}}$, can be defined in terms of $\{Z_l\}_{l=1}^L$ [22, (4.1)]

$$D_{\lambda_{\rm th}}=\sum_{l=2}^L\left(Z_l-Z_{l-1}\right)^2, \quad (22)$$

which includes both up- and down-crossings.

After some simple manipulations, the expected crossing rate at the level $\lambda_{\rm th}$ can be written as

$$\frac{\mathbb{E}[D_{\lambda_{\rm th}}]}{(L-1)T_s}=\frac{2P_r\{Z_l=1\}-2P_r\{Z_l=1,Z_{l-1}=1\}}{T_s}. \quad (23)$$

Therefore the expected down crossing rate at $\lambda_{\rm th}$, denoted by $N_\lambda(\lambda_{\rm th})$, is half of (23), given by

$$N_\lambda(\lambda_{\rm th})=\frac{P_r\{Z_l=1\}-P_r\{Z_l=1,Z_{l-1}=1\}}{T_s}. \quad (24)$$

To simplify the notation, we use ϕ for $P_r\{Z_l=1\}$ and $\varphi(\varrho_1)$ to denote $P_r\{Z_l=1,Z_{l-1}=1\}$, where $\varrho_1=|\rho_h(T_s)|$, defined before, i.e.,

$$\varrho_1=\left|\sum_{n=1}^N P_n\frac{I_0\left(\sqrt{\kappa_n^2-4\pi^2 f_D^2T_s^2+\jmath 4\pi\kappa_n f_D T_s\cos\theta_n}\right)}{I_0(\kappa_n)}\right|. \quad (25)$$

ϕ and $\varphi(\varrho_1)$ can be calculated as follows

$$\begin{aligned}\phi=P_r\{X\geq\lambda_{\rm th}\}&=\int_{\lambda_{\rm th}}^\infty\left(\frac{x^2}{2}-x+1\right)e^{-x}\mathrm{d}x,\\ &=e^{-\lambda_{\rm th}}\left(1+\frac{\lambda_{\rm th}^2}{2}\right),\end{aligned} \quad (26)$$

and

$$\varphi(\varrho_1)=P_r\{X\geq\lambda_{\rm th},Y\geq\lambda_{\rm th}\}, \quad (27)$$

which simplifies to (12), with $\Gamma(a,z)=\int_z^\infty t^{a-1}e^{-t}\mathrm{d}t$ [18, pp. 949, 8.350.2] as the upper incomplete gamma function, by applying (5) and (14) to (27).

$$\varphi(\varrho_1)=\frac{\left(1-\varrho_1^2\right)^3}{4\varrho_1^2}\sum_{k=0}^{\infty}\frac{\varrho_1^{2k}}{(k!)^2}\left\{\frac{\varrho_1^2}{(1-\varrho_1^2)^2}\Gamma^2\!\left(k+1,\frac{\lambda_{\text{th}}}{1-\varrho_1^2}\right)+\left[\frac{1}{1-\varrho_1^2}\Gamma\!\left(k+1,\frac{\lambda_{\text{th}}}{1-\varrho_1^2}\right)-\Gamma\!\left(k+2,\frac{\lambda_{\text{th}}}{1-\varrho_1^2}\right)\right]^2\right\}$$
$$+e^{-2\lambda_{\text{th}}}\left[\frac{1}{2}-\frac{\lambda_{\text{th}}^2}{4}\left(\varrho_1-\frac{1}{\varrho_1}\right)^2\right] \tag{12}$$

By plugging (26) and (27) into (24), we obtain the expected crossing rate at the level λ_{th} as

$$\boxed{N_\lambda(\lambda_{\text{th}})=\frac{e^{-\lambda_{\text{th}}}\left(1+\frac{\lambda_{\text{th}}^2}{2}\right)-\varphi(\varrho_1)}{T_s},} \tag{28}$$

where $\varphi(\varrho_1)$ is given in (12).

B. AFD of an Eigen-Channel

The cumulative distribution function (CDF) of $\lambda(lT_s), \forall l$ is obtained as

$$F_\lambda(\lambda_{\text{th}})=P_r\left\{X\le\lambda_{\text{th}}\right\}=1-\phi=1-e^{-\lambda_{\text{th}}}\left(1+\frac{\lambda_{\text{th}}^2}{2}\right), \tag{29}$$

where ϕ comes from (26).

The AFD of an *eigen*-channel is therefore given by

$$\boxed{\bar{t}_\lambda(\lambda_{\text{th}})=\frac{F_\lambda(\lambda_{\text{th}})}{N_\lambda(\lambda_{\text{th}})}=\frac{\left[1-e^{-\lambda_{\text{th}}}\left(1+\frac{\lambda_{\text{th}}^2}{2}\right)\right]T_s}{e^{-\lambda_{\text{th}}}\left(1+\frac{\lambda_{\text{th}}^2}{2}\right)-\varphi(\varrho_1)},} \tag{30}$$

where $\varphi(\varrho_1)$ is given in (12).

VI. Numerical Results and Discussion

In this paper, a generic power spectrum [16, (8)] is used to simulate Rayleigh flat fading channels with *non-isotropic* scattering, according to the spectral method [23]. To verify the accuracy of the derived formulas, we consider two types of scattering environments: *isotropic* scattering, and *non-isotropic* scattering with three clusters of scatterers. For the *non-isotropic* scattering, parameters of three clusters, $[P_n,\kappa_n,\theta_n], n=1,2,3$, are given by $[P_1,\kappa_1,\theta_1]=\left[0.45,2,\frac{\pi}{18}\right]$, $[P_2,\kappa_2,\theta_2]=\left[0.2,20,\frac{11\pi}{18}\right]$, and $[P_3,\kappa_3,\theta_3]=\left[0.35,3,\frac{53\pi}{36}\right]$, respectively. In addition, in all the simulations, the maximum Doppler frequency f_D is set to 1Hz, and $T_s=\frac{1}{20f_D}$ seconds[4].

In the following subsections, simulations are performed to verify NACF, correlation coefficient, LCR and AFD of an *eigen*-channel of a 2×2 MIMO system, in the above two propagation environments.

A. Isotropic Scattering

This is Clarke's model [10], with uniform AoA. The simulation results are shown in Fig. 2.

[4]Note that the value of f_D is has just a scaling effect, $f_D=1$ Hz is chosen to make the simulations faster.

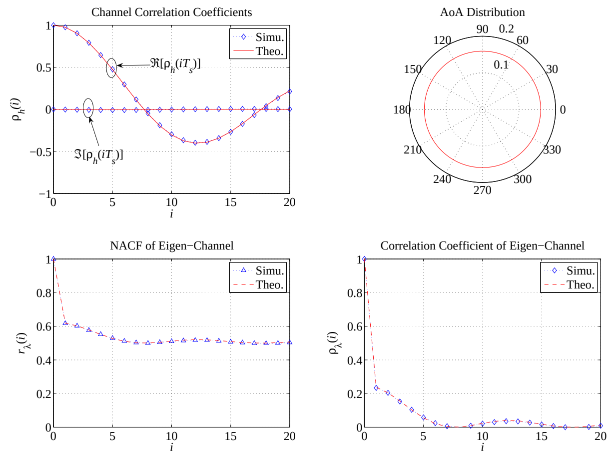

Fig. 2. The channel correlation coefficient, AoA distribution, as well as NACF and correlation coefficient of an *eigen*-channel, in a 2×2 MIMO system with *isotropic* scattering.

B. Non-isotropic Scattering

This is a general case, with an arbitrary AoA distribution. Simulations are carried out, with the results shown in Fig. 3.

In Figs. 2-3, the upper left and right figures show the channel correlation coefficient and AoA distributions, and the lower left and right figures show NACF and correlation coefficient of an *eigen*-channel $\lambda(lT_s), l\in[1,L]$, respectively. In all the figures, "Simu." means simulation, whereas "Theo." means the theoretical channel coefficient, NACF and corre-

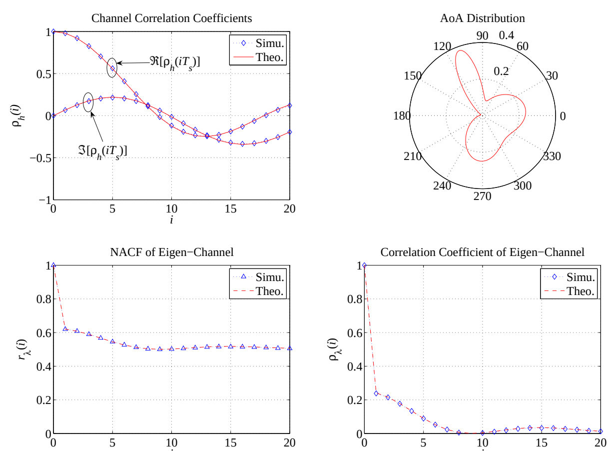

Fig. 3. The channel correlation coefficient, AoA distribution, as well as NACF and correlation coefficient of an *eigen*-channel, in a 2×2 MIMO system with *non-isotropic* scattering.

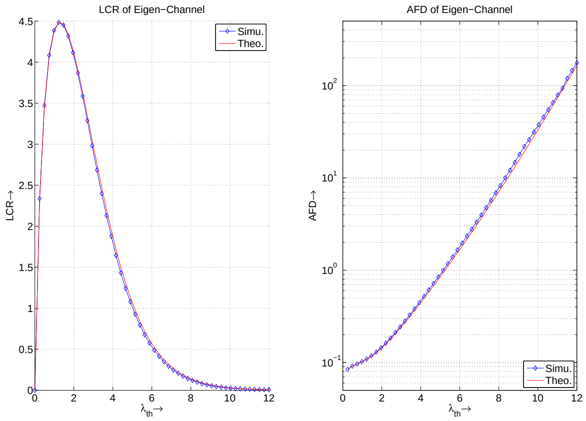

Fig. 4. LCR and AFD of an *eigen*-channel, in a 2×2 MIMO system with *isotropic* scattering.

lation coefficient, calculated according to (6), (17) and (18), respectively.

In Figs. 4-5, the left and right figures show LCR and AFD, respectively, where "Theo." refers to the theoretical LCR and AFD, calculated according to (28) and (30), respectively. From Figs. 4-5, it is clear to see that both LCR and AFD are not sensitive to the propagation environments. This is because LCR and AFD only depend on ϱ_1 (r.f. Eqs. (28) and (30)), the amplitude of the channel correlation coefficient evaluated at $\tau = T_s$.

From Figs. 2-5, one can say that for both types of scattering, the theoretical formulas perfectly match the simulation results.

VII. Conclusion

In this paper, closed-form expressions for the autocorrelation function, correlation coefficient, level crossing rate and average fade duration of an *eigen*-channel are derived, for a 2×2 MIMO time-varying Rayleigh flat fading channel. The analytical expressions, supported by Monte Carlo simulations, provide useful qualitative and quantitative information regarding the fluctuations of MIMO channels.

Although we only considered 2×2 MIMO systems, it is straightforward to use the techniques developed in this paper to deal with other MIMO systems with $N_T > 2$ transmitters and $N_R > 2$ receivers, where all the subchannels are independent and identically distributed, with the same temporal correlation function.

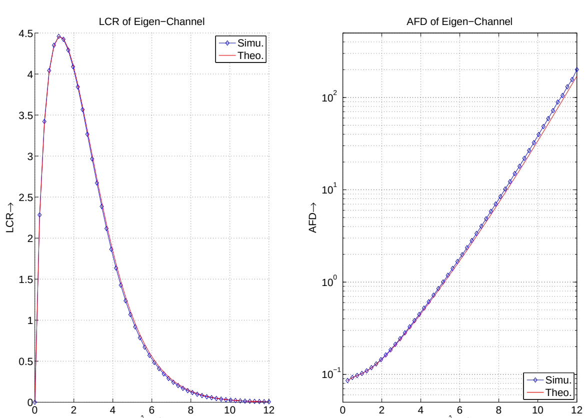

Fig. 5. LCR and AFD of an *eigen*-channel, in a 2×2 MIMO system with *non-isotropic* scattering.

References

[1] G. J. Foschini and M. J. Gans, "On limits of wireless communications in a fading environment when using multiple antennas," *Wireless Personal Commun.*, vol. 6, pp. 311–335, 1998.

[2] İ. E. Telatar, "Capacity of multi-antenna Gaussian channels," *European Trans. Telecommun.*, vol. 10, pp. 585–595, 1999.

[3] D. W. Bliss, A. M. Chan, and N. B. Chang, "MIMO wireless communication channel phenomenology," *IEEE Trans. Antennas Propagat.*, vol. 52, pp. 2073–2082, Aug. 2004.

[4] M. T. Ivrlač, W. Utschick, and J. A. Nossek, "Fading correlations in wireless MIMO communication systems," *IEEE J. Select. Areas Commun.*, vol. 21, pp. 819–828, June 2004.

[5] J. Maurer, C. Waldschmidt, T. Kayser, and W. Wiesbeck, "Characterisation of the time-dependent urban MIMO channel in FDD communication systems," in *Proc. IEEE Veh. Technol. Conf.*, Jeju, Korea, 2003, pp. 544–548.

[6] G. Lebrun, J. Gao, and M. Faulkner, "MIMO transmission over a time-varying channel using SVD," *IEEE Trans. Wireless Commun.*, vol. 4, pp. 757–764, Mar. 2005.

[7] H. Sampath, P. Stoica, and A. Paulraj, "Generalized linear precoder and decoder design for MIMO channels using the weighted MMSE criterion," *IEEE Trans. Commun.*, vol. 49, pp. 2198–2206, Dec. 2001.

[8] S. K. Jayaweera and H. V. Poor, "Capacity of multiple-antenna systems with both receiver and transmitter channel state information," *IEEE Trans. Inform. Theory*, vol. 49, pp. 2697–2709, Oct. 2003.

[9] D. Tse and P. Viswanath, *Fundamentals of Wireless Communication*. Cambridge, UK: Cambridge University Press, 2005.

[10] W. C. Jakes, Ed., *Microwave Mobile Communications*. New York: IEEE Press, 1994.

[11] A. Abdi, K. Wills, H. A. Barger, M. S. Alouini, and M. Kaveh, "Comparison of the level crossing rate and average fade duration of Rayleigh, Rice, and Nakagami fading models with mobile channel data," in *Proc. IEEE Veh. Technol. Conf.*, Boston, MA, 2000, pp. 1850–1857.

[12] N. Youssef, T. Munakata, and M. Takeda, "Fade statistics in Nakagami fading environments," in *Proc. IEEE Int. Symp. Spread Spec. Tech. App.*, Mainz, Germany, 1996, pp. 1244–1247.

[13] A. Abdi, J. A. Barger, and M. Kaveh, "A parametric model for the distribution of the angle of arrival and the associated correlation function and power spectrum at the mobile station," *IEEE Trans. Veh. Technol.*, vol. 51, pp. 425–434, May 2002.

[14] A. Abdi, W. C. Lau, M. S. Alouini, and M. Kaveh, "A new simple model for land mobile satellite channels: First- and second-order statistics," *IEEE Trans. Wireless Commun.*, vol. 2, pp. 519–528, May 2003.

[15] L. H. Ozarow, S. Shamai, and A. D. Wyner, "Information theoretic considerations for cellular mobile radio," *IEEE Trans. Veh. Technol.*, vol. 43, pp. 359–378, May 1994.

[16] S. Wang and A. Abdi, "On the second-order statistics of the instantaneous mutual information of time-varying fading channels," in *Proc. IEEE Int. Workshop Signal Processing Advances in Wireless Communications*, New York, 2005, pp. 405–409.

[17] ——, "Joint singular value distribution of two correlated rectangular complex Gaussian matrices and its application," submitted to *SIAM J. Matrix Anal. Appl.*, Feb. 2006. [Online]. Available: http://arxiv.org/abs/math.PR/0603170

[18] I. S. Gradshteyn, I. M. Ryzhik, and A. Jeffrey, Eds., *Table of Integrals, Series, and Products*, 5th ed. San Diego, CA: Academic, 1994.

[19] M. K. Simon, *Probability Distributions Involving Gaussian Random Variables: A Handbook for Engineers and Scientists*. Boston, MA: Kluwer, 2002.

[20] S. Wang, "Envelope correlation coefficient for logarithmic diversity receivers revisited," submitted to *IEEE Trans. Commun.*, Feb. 2006.

[21] W. B. Davenport and W. L. Root, *An Introduction to the Theory of Random Signals and Noise*. New York: Wiley, 1987.

[22] B. Kedem, *Time Series Analysis by Higher Order Crossings*. New York: IEEE Press, 1994.

[23] K. Acolatse and A. Abdi, "Efficient simulation of space-time correlated MIMO mobile fading channels," in *Proc. IEEE Veh. Technol. Conf.*, Orlando, FL, 2003, pp. 652–656.